

Quasinormal modes of scalarized black holes in the Einstein-Maxwell-Scalar theory

Yun Soo Myung^{a*} and De-Cheng Zou^{a,b†}

^aInstitute of Basic Sciences and Department of Computer Simulation, Inje University
Gimhae 50834, Korea

^bCenter for Gravitation and Cosmology and College of Physical Science and Technology,
Yangzhou University, Yangzhou 225009, China

Abstract

We perform the stability analysis on scalarized charged black holes in the Einstein-Maxwell-Scalar (EMS) theory by computing quasinormal mode spectrum. It is noted that the appearance of these black holes with scalar hair is closely related to the instability of Reissner-Nordström black holes without scalar hair in the EMS theory. The scalarized charged black hole solutions are classified by the order number of $n = 0, 1, 2, \dots$, where $n = 0$ is called the fundamental branch and $n = 1, 2, \dots$ denote the n excited branches. Here, we show that the $n = 1, 2$ excited black holes are unstable against the $s(l = 0)$ -mode scalar perturbation, while the $n = 0$ black hole is stable against all scalar-vector-tensor perturbations. This is consistent with other scalarized black holes without charge found in the Einstein-Scalar-Gauss-Bonnet theory.

*e-mail address: ysmyoung@inje.ac.kr

†e-mail address: dczou@yzu.edu.cn

1 Introduction

Recently, a scalarization of the Reissner-Nordström (RN) black holes was investigated in the Einstein-Maxwell-scalar (EMS) theory which is a simpler theory than the Einstein-Scalar-Gauss-Bonnet-scalar (ESGB) theory [1]. Here, $q = Q/M$ may increase beyond unity, compared to $0 < q \leq 1$ for the RN black hole. The EMS theory is a second-order theory which includes three propagating modes of scalar, vector, and tensor. In this case, the instability of RN black hole was determined solely by the linearized scalar equation because the RN black hole is stable against tensor-vector perturbations theory [2, 3, 4, 5]. It is shown that the appearance of the scalarized charged black hole is closely associated with the Gregory-Laflamme (GL) instability of the RN black hole without scalar hair [6]. A difference with the ESGB theory [7] is that there is no scalarization bands in the EMS theory, implying no upper bound on the coupling constant α as the $n = 0(\alpha \geq 8.019)$, $1(\alpha \geq 40.84)$, $2(\alpha \geq 99.89)$, \dots scalarized charged black holes.

The scalarized black holes without charge have been found from the ESGB theories [7, 8, 9]. It is emphasized that these black holes with scalar hair are connected to the appearance of instability for the Schwarzschild black hole without scalar hair. We note that the instability of Schwarzschild black hole in ESGB theory is considered as not the tachyonic instability but the GL instability [10] when comparing it with the GL instability of the Schwarzschild black hole in the Einstein-Weyl gravity [11]. Here, the notion of the GL instability comes from the three observations [12, 13, 14, 15]: i) The instability is based on the $s(l = 0)$ -mode perturbation for either massive scalar or massive tensor. ii) The perturbed equation should include an effective mass term, so that the potential $V(r)$ develops negative region near the horizon of black hole but it becomes positive just after crossing the r -axis, leading to $\int_{r_+}^{\infty} dr[V(r)/f(r)] > 0$ with the metric function $f(r)$. Actually, this corresponds to a weaker condition than the sufficient condition of instability ($\int_{r_+}^{\infty} dr[V(r)/f(r)] < 0$) including the tachyonic instability because the integral of potential may be positive. iii) The instability of a black hole without hair is closely related to the appearance of a newly black hole with hair where the hair is defined by non-zero scalar outside and on the horizon.

Concerning the stability of scalarized black holes, it turns out that the $n = 0$ black hole is stable against all perturbations, while $n = 1, 2, \dots$ black holes are unstable against the $l = 0(s\text{-mode})$ scalar perturbation in the Einstein-Born-Infeld-scalar theory [16] and the ESGB theory [17]. The former was based on the scalar perturbation only, while the

latter was based on the spherically symmetric tensor perturbations including the scalar perturbation. For the stability of scalarized charged black hole in the EMS theory, the $n = 0$ black hole was mentioned within the scalar perturbation [1].

In this work, we wish to carry out the stability analysis on the scalarized charged black holes in the EMS theory by computing quasinormal mode spectrum. We wish to employ the full tensor-vector-scalar perturbations splitting into the axial and polar parts. Observing the potentials around the $n = 0, 1, 2$ black holes with $q = 0.7$ and together with computing quasinormal frequencies of the five physically propagating modes, we will find that the $n = 0$ black hole is stable against all perturbations, while $n = 1, 2$ black holes are unstable against the $l = 0$ (s -mode) scalar perturbation in the EMS theory.

2 Scalarized charged black holes

We start by mentioning the action of EMS theory without scalar potential [1]

$$S_{\text{EMS}} = \frac{1}{16\pi} \int d^4x \sqrt{-g} \left[R - 2\partial_\mu \phi \partial^\mu \phi - e^{\alpha\phi^2} F^2 \right], \quad (1)$$

where ϕ is a scalar field, α is a Maxwell-scalar coupling constant as a mass-like parameter, and $F^2 = F_{\mu\nu} F^{\mu\nu}$ is the Maxwell kinetic term. In this work, we do not consider the Einstein-Maxwell-dilaton theory with a usual coupling of $e^{\alpha\phi}$ [18, 19]. The EMS theory describes three of a massive scalar, a massless vector, and a massless tensor which lead to five ($1+2+2=5$) physically dynamical modes propagating on the scalarized charged black hole background.

We derive the Einstein equation from the action (1)

$$G_{\mu\nu} = 2\partial_\mu \phi \partial_\nu \phi - (\partial\phi)^2 g_{\mu\nu} + 2T_{\mu\nu} \quad (2)$$

with $G_{\mu\nu} = R_{\mu\nu} - (R/2)g_{\mu\nu}$ and $T_{\mu\nu} = e^{\alpha\phi^2} (F_{\mu\rho} F_\nu{}^\rho - F^2 g_{\mu\nu}/4)$. The Maxwell equation takes the form

$$\nabla^\mu F_{\mu\nu} - 2\alpha\phi \nabla^\mu(\phi) F_{\mu\nu} = 0. \quad (3)$$

Importantly, the scalar equation is given by

$$\square\phi - \frac{\alpha}{2} e^{\alpha\phi^2} F^2 \phi = 0. \quad (4)$$

For our purpose, we introduce the metric ansatz as [1]

$$ds^2 = \bar{g}_{\mu\nu} dx^\mu dx^\nu = -N(r)e^{-2\delta(r)} dt^2 + \frac{dr^2}{N(r)} + r^2(d\theta^2 + \sin^2\theta d\varphi^2) \quad (5)$$

with a metric function $N(r) = 1 - 2m(r)/r$, in addition to $U(1)$ potential $\bar{A} = v(r)dt$ and scalar $\bar{\phi}(r)$. We would like to mention that the RN black hole solution [$\tilde{N}(r) = 1 - 2M/r + Q^2/r^2, \delta(r) = \bar{\phi}(r) = 0$] is defined, irrespective of any value of α . However, a scalarized charged black hole is defined by restricting an allowable range for α . The threshold of instability for a RN black hole is closely related to the appearance of the $\alpha \geq 8.019$ fundamental branch which is identified with the $n = 0$ scalarized charged black hole. Also, the static scalar perturbation around the RN black hole indicates the appearance of $n = 1, 2 \dots$ scalarized charged black holes.

First of all, we consider the static scalar perturbed equation [$(\tilde{\nabla}^2 - \alpha\tilde{F}^2/2)\delta\phi = 0$] with $\delta\phi = Y_{lm}(\theta, \varphi)\varphi_l(r)$ on the RN black hole background to identify how the $n = 0, 1, 2$ black holes come out as

$$\frac{1}{r^2} \frac{d}{dr} \left[r^2 \tilde{N}(r) \frac{d\varphi_l(r)}{dr} \right] - \left[\frac{l(l+1)}{r^2} - \frac{\alpha Q^2}{r^4} \right] \varphi_l(r) = 0 \quad (6)$$

which describes an eigenvalue problem in the radial direction: for a given $l = 0$, requiring an asymptotically vanishing, smooth scalar field selects a discrete set of $n = 0, 1, 2, \dots$. Actually, these determine the bifurcation points of scalar solution as $\alpha_n(q = 0.7) = \{8.019, 40.84, 99.89, \dots\}$. In Fig. 1, these solutions are classified by the node number n for $\varphi(z) = \varphi_{l=0}(z)$ with $z = r/(2M)$. Furthermore, n denotes the order number for classifying different branches of scalarized black holes.

Now, we focus on looking for a scalarized charged black hole with $q = Q/M = 0.7$. Plugging (5) into (2)-(4), one has the four equations

$$-2m'(r) + e^{2\delta(r)+\alpha(\bar{\phi}(r))^2} r^2 (v'(r))^2 + [r^2 - 2rm(r)](\bar{\phi}'(r))^2 = 0, \quad (7)$$

$$\delta'(r) + r(\bar{\phi}'(r))^2 = 0, \quad (8)$$

$$v'(r) \left(2 + r\delta'(r) + 2r\alpha\bar{\phi}(r)\bar{\phi}'(r) \right) + rv''(r) = 0, \quad (9)$$

$$e^{2\delta(r)+\alpha(\bar{\phi}(r))^2} r^2 \alpha \bar{\phi}(r) (v'(r))^2 + r[r - 2m(r)]\bar{\phi}''(r) - \left(m(r)[2 - 2r\delta'(r)] + r[-2 + r + 2m'(r)]\delta'(r) \right) \bar{\phi}'(r) = 0, \quad (10)$$

where the prime ($'$) denotes differentiation with respect to its argument. From (9), one has a relation of $v' = -e^{-\delta-\alpha\bar{\phi}^2} Q^2/r$. Considering an outer horizon located at $r = r_+ = 0.857$

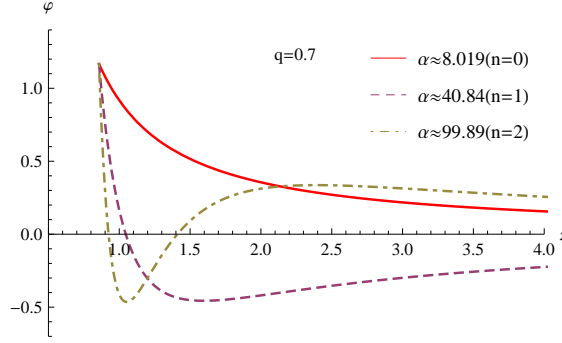


Figure 1: Radial profiles of $\varphi(z) = \varphi_{l=0}(z)$ as function of $z = r/(2M)$ for the first three perturbed scalar solutions on the RN black hole with $q = 0.7$. Here n represents the number of nodes for $\varphi(z)$ and it denotes the order number for labeling scalarized black holes on later.

in the RN black hole, one finds a numerical solution to four equations in the near-horizon

$$m(r) = \frac{r_+}{2} + m_1(r - r_+) + \dots, \quad (11)$$

$$\delta(r) = \delta_0 + \delta_1(r - r_+) + \dots, \quad (12)$$

$$\bar{\phi}(r) = \phi_0 + \phi_1(r - r_+) + \dots, \quad (13)$$

$$v(r) = v_1(r - r_+) + \dots, \quad (14)$$

where the coefficients are determined by

$$m_1 = \frac{e^{-\alpha\phi_0^2}Q^2}{2r_+^2}, \quad \delta_1 = -r_+\phi_1^2, \quad \phi_1 = \frac{\alpha\phi_0Q^2}{r_+(Q^2 - e^{\alpha\phi_0^2}r_+^2)}, \quad v_1 = -\frac{e^{-\delta_0 - \alpha\phi_0^2}Q}{r_+^2}. \quad (15)$$

This near-horizon solution involves two parameters of $\phi_0 = \bar{\phi}(r_+, \alpha)$ and $\delta_0 = \delta(r_+, \alpha)$, which will be determined by matching (11)-(14) with the asymptotic solution in the far-region

$$\begin{aligned} m(r) &= M - \frac{Q^2 + Q_s^2}{2r} + \dots, \quad \bar{\phi}(r) = \frac{Q_s}{r} + \dots, \\ \delta(r) &= \frac{Q_s^2}{2r^2} + \dots, \quad v(r) = \Phi + \frac{Q}{r} + \dots, \end{aligned} \quad (16)$$

which include the scalar charge Q_s and the electrostatic potential Φ .

As a concrete scalarized black hole solution with $q = 0.7$, we display the two numerical solutions [metric function $N(r)$ only] with the coupling constant $\alpha = 8.083, 48$ locating

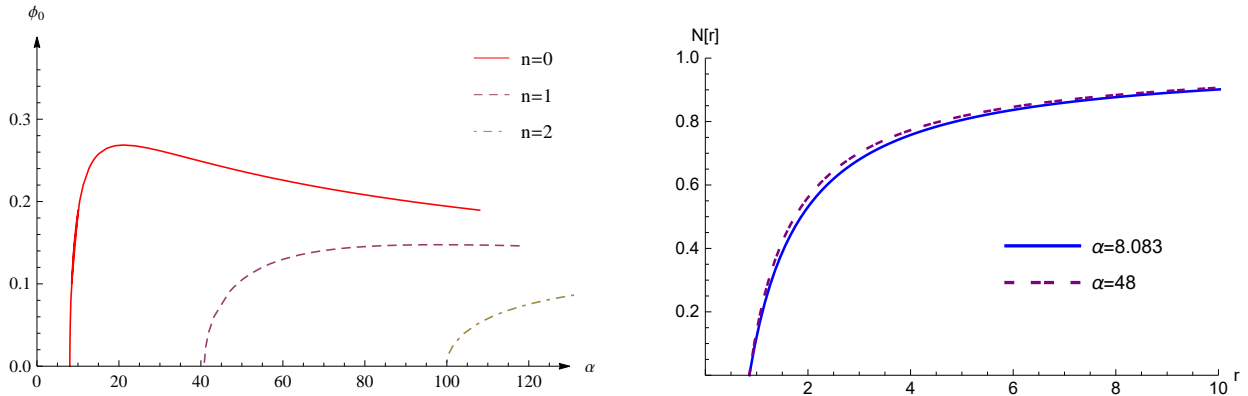


Figure 2: (Left) The scalar field $\phi_0 = \bar{\phi}(r_+)$ at the horizon as function of α . The $n = 0$ fundamental branch starts from the first bifurcation point at $\alpha = 8.019$, while $n = 1, 2$ excited branches start from the second point at $\alpha = 40.84$ and the third point at $n = 99.89$. (Right) The scalarized charged black hole solutions for the $n = 0(\alpha \geq 8.019)$ fundamental branch. Here we display two metric functions $N(r)$ with $\alpha = 8.083$ and 48 residing in the $n = 0$ fundamental branch.

on the $n = 0(\alpha \geq 8.019)$ fundamental branch in Fig. 2. It is worth noting that the $n = 1(\alpha \geq 40.84)$, $2(\alpha \geq 99.89)$ excited branch solutions take the similar forms as the $n = 0$ case. For simple notation, we call these scalarized charged black holes as the $n = 0, 1, 2, \dots$ black holes.

At this stage we mention that our choice of $q = 0.7$ is nothing special, but it is chosen for a non-extremal black hole between the Schwarzschild ($q = 0$) and the extremal black holes. When the charge q is bigger (smaller) than $q = 0.7$, one expects to find similar solutions and quasinormal modes. Hence, we will perform the stability analysis on the $n = 0, 1, 2$ black hole solutions with $q = 0.7$ in the next section. Although the $n > 2$ black holes exist, it is expected that they show similar features as the $n = 1, 2$ black holes show.

3 Linearized equations

We consider the perturbed fields around the background quantities

$$g_{\mu\nu} = \bar{g}_{\mu\nu} + h_{\mu\nu}, \quad A_\mu = \bar{A}_\mu + a_\mu, \quad \phi = \bar{\phi} + \delta\phi. \quad (17)$$

Plugging (17) into Eqs.(2)-(4) leads to complicated linearized equations. Considering ten degrees of freedom for $h_{\mu\nu}$, four for a_μ , and one for $\delta\phi$ initially, the EMS theory describing a massive scalar and massless vector-tensor propagations provides five (1+2+2=5) physically propagating modes on the black hole background. The stability analysis should be based on these physically propagating fields as the solutions to the linearized equations. In a spherically symmetric background (5), the perturbations can be decomposed into spherical harmonics $Y_l^m(\theta, \varphi)$ with multipole index l and azimuthal number m . This decomposition splits the tensor-vector perturbations into ‘‘axial (A)’’ which acquires a factor $(-1)^{l+1}$ under parity inversion and ‘‘polar (P)’’ which acquires a factor $(-1)^l$.

We expand the metric perturbations in tensor spherical harmonics under the Regge-Wheeler gauge. For the axial part with two modes h_0 and h_1 , the perturbed metric takes the form

$$h_{\mu\nu}^A(t, r, \theta, \varphi) = \int d\omega e^{-i\omega t} \sum_{l,m} \begin{bmatrix} 0 & 0 & -\frac{h_0(r)\partial_\varphi Y_l^m}{\sin\theta} & h_0(r) \sin\theta \partial_\theta Y_l^m \\ * & 0 & -\frac{h_1(r)\partial_\varphi Y_l^m}{\sin\theta} & h_1(r) \sin\theta \partial_\theta Y_l^m \\ * & * & 0 & 0 \\ * & * & * & 0 \end{bmatrix}, \quad (18)$$

where asterisks denote symmetrization. For polar perturbations with four modes (H_0, H_1, H_2, K), we have

$$h_{\mu\nu}^P = \int d\omega e^{-i\omega t} \sum_{l,m} \begin{bmatrix} H_0(r)e^{-2\delta(r)}N(r) & H_1(r) & 0 & 0 \\ * & \frac{H_2(r)}{N(r)} & 0 & 0 \\ * & * & r^2K(r) & 0 \\ * & * & * & r^2 \sin^2\theta K(r) \end{bmatrix} Y_l^m. \quad (19)$$

On the other hand, we decompose the vector perturbations into

$$a_\mu^A = \int d\omega e^{-i\omega t} \sum_{l,m} \left[0, 0, -\frac{u_4(r)\partial_\varphi Y_l^m}{\sin\theta}, u_4(r) \sin\theta \partial_\theta Y_l^m \right] \quad (20)$$

and

$$a_\mu^P = \int d\omega e^{-i\omega t} \sum_{l,m} \left[\frac{u_1(r)Y_l^m}{r}, \frac{u_2(r)Y_l^m}{rN(r)}, 0, 0 \right], \quad (21)$$

where we gauge $a_{\theta,\varphi}^P$ away. Lastly, we have a polar scalar perturbation as

$$\delta\phi = \int d\omega e^{-i\omega t} \sum_{l,m} \delta\phi_1(r) Y_l^m. \quad (22)$$

The linearized equations could be split into axial and polar parts.

In general, the axial part is composed of two coupled equations for Maxwell $\hat{F}(u_4)$ and Regge-Wheeler $\hat{K}(h_0, h_1)$,

$$\left[\frac{d^2}{dr_*^2} + \omega^2 \right] \hat{F}(r) = V_{\text{FF}}^{\text{A}}(r) \hat{F}(r) + V_{\text{FK}}^{\text{A}}(r) \hat{K}(r), \quad (23)$$

$$\left[\frac{d^2}{dr_*^2} + \omega^2 \right] \hat{K}(r) = V_{\text{KF}}^{\text{A}}(r) \hat{F}(r) + V_{\text{KK}}^{\text{A}}(r) \hat{K}(r), \quad (24)$$

where the potentials are given by

$$V_{\text{FF}}^{\text{A}}(r) = \frac{N}{r^2 e^{2\delta}} \left[e^{2\delta + \alpha \bar{\phi}^2} r^2 (4 - \alpha \bar{\phi}^2) (v')^2 + l(l+1) + \alpha r N \bar{\phi}' (r(1 + \alpha \bar{\phi}^2) \bar{\phi}' - 2\bar{\phi}) \right] \quad (25)$$

$$V_{\text{FK}}^{\text{A}}(r) = V_{\text{KF}}^{\text{A}}(r) = -\frac{2e^{-\delta + \alpha \bar{\phi}^2/2} (l-1)(l+2) N v'}{r}, \quad (26)$$

$$V_{\text{KK}}^{\text{A}}(r) = \frac{N}{r^2 e^{2\delta}} \left[(l-1)(l+2) - r N' + N(2 + r\delta) \right]. \quad (27)$$

Here the tortoise coordinate $r_* \in (-\infty, \infty)$ is defined by the relation of $dr_*/dr = e^\delta/N$. At this stage, it is worth noting that in the limits of $\bar{\phi} = \delta = 0$, $V_{\text{FF}}^{\text{A}}(r)$, $V_{\text{FK}}^{\text{A}}(r)$, and $V_{\text{KK}}^{\text{A}}(r)$ recovers those for the RN black hole in the EM theory [20]. In addition, we would like to mention that the diagonalized forms may be adopted to compute quasinormal modes propagating around scalarized charged black holes. However, it is not easy to find a simple method to diagonalize two coupled equations (23) and (24). Actually, the diagonalization is not easily performed because of the presence of the background scalar. Instead, we will derive the quasinormal modes propagating around scalarized charged black holes by solving the two coupled equations directly.

On the other hand, the polar part is composed of six coupled equations for Zerilli,

Maxwell, and scalar as

$$K'(r) = - \left(\frac{l(l+1) + 2N + 2rN' - 2}{2r^2} + e^{2\delta + \alpha\bar{\phi}^2} v'^2 + N\phi'(r)^2 \right) H_1(r) \quad (28)$$

$$\frac{H_0(r)}{r} + \left(\frac{N'}{2N} - \frac{1}{r} - \delta' \right) K(r) - \frac{2\bar{\phi}'}{r} \delta\phi_1(r),$$

$$H_1'(r) = - \frac{4ie^{\alpha\bar{\phi}^2} v'}{\omega} f_{12}(r) - \frac{H_0(r) + K(r)}{N} + \left(\delta' - \frac{N'}{N} \right) H_1(r), \quad (29)$$

$$H_0'(r) = \left(\frac{1}{r} + 2\delta' - \frac{N'}{N} \right) [H_0(r) - K(r)] + \frac{4e^{2\delta + \alpha\bar{\phi}^2} v'}{N} f_{02}(r) + \frac{2\bar{\phi}'}{r} \delta\phi_1(r) \quad (30)$$

$$+ \left(\frac{e^{2\delta} \omega^2}{N} - e^{2\delta + \alpha\bar{\phi}^2} v'^2 - N\phi'^2 - \frac{l(l+1)}{2r^2} - \frac{N + rN' - 1}{r^2} \right) H_1(r),$$

$$f_{02}'(r) = v'K(r) + \frac{2\alpha\bar{\phi}V'}{r} \delta\phi_1(r) + \left(\frac{l(l+1)ie^{-2\delta}N}{r^2\omega} - i\omega \right) f_{12}(r), \quad (31)$$

$$f_{12}'(r) = - \frac{i\omega e^{2\delta}}{N^2} f_{02}(r) + \left(\delta' - 2\alpha\bar{\phi}\bar{\phi}' - \frac{N'}{N} \right) f_{12}(r), \quad (32)$$

$$\delta\phi_1''(r) = \left[\frac{l(l+1)}{r^2N} - \frac{e^{2\delta}\omega^2}{N^2} + \frac{N' + e^{2\delta + \alpha\bar{\phi}^2} r\alpha(2\alpha\bar{\phi}^2 - 1)v'^2 - N(\delta' - 4r\bar{\phi}'^2)}{rN} \right] \delta\phi_1(r)$$

$$+ \left(\delta' - \frac{N'}{N} \right) \delta\phi_1'(r) + \frac{2ie^{\alpha\bar{\phi}^2} \alpha\bar{\phi}v'}{r\omega} f_{12}(r) + \frac{4e^{2\delta + \alpha\bar{\phi}^2} rv'\bar{\phi}}{N} f_{02}(r) \quad (33)$$

$$- \frac{r \left(e^{2\delta + \alpha\bar{\phi}^2} \alpha\bar{\phi}v'^2 + (N' - 2N\delta')\bar{\phi}' \right)}{N} H_0(r) + \frac{2re^{2\delta + \alpha\bar{\phi}^2} \alpha\bar{\phi}v'^2}{N} K(r).$$

Here we have $H_2(r) = H_0(r)$, $f_{12}(r) = \frac{u_2(r)}{rN(r)}$ and $f_{02}(r) = \frac{u_1(r)}{r}$. Interestingly, these coupled equations describe three physically propagating modes.

4 Stability Analysis

The stability analysis will be performed by getting quasinormal frequency of $\omega = \omega_r + i\omega_i$ when solving the linearized equations with appropriate boundary conditions at the outer horizon: ingoing waves and at infinity: purely outgoing waves. Also, the late-time signals from perturbed black holes are dominated by the fundamental quasinormal mode, which corresponds to the mode with smallest imaginary component. We will compute the lowest quasinormal modes of the scalarized black holes by making use of the fully numerical background and the linearized equations (23)-(24) for axial part and the linearized equations

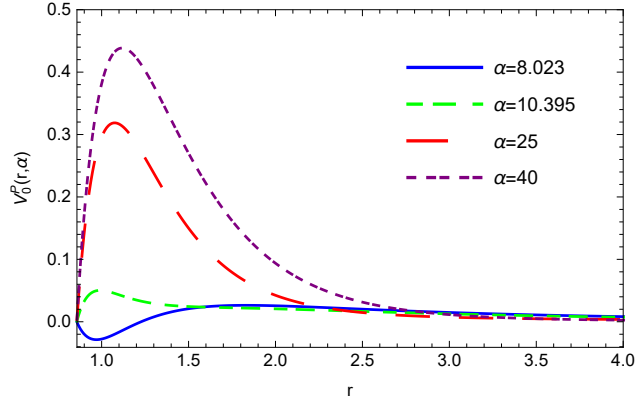


Figure 3: Four scalar potential graphs $V_0^P(r, \alpha)$ with $l = 0$ around the $n = 0$ ($\alpha \geq 8.019$) black hole. The whole potentials are positive definite except that the $\alpha = 8.083$ case having negative region near the horizon.

(28)-(33) for polar part. To compute the quasinormal modes, we use a direct-integration method [21].

Usually, a positive definite potential $V(r)$ without any negative region guarantees the stability of black hole. On the other hand, a sufficient condition for instability is given by $\int_{r_+}^{\infty} dr [e^{\delta} V(r)/N(r)] < 0$ [22] in accordance with the existence of the unstable modes. However, some potentials with negative region near the outer horizon whose integral is positive ($\int_{r_+}^{\infty} dr [e^{\delta} V(r)/N(r)] > 0$) do not imply a definite instability. To determine the instability of the $n = 0, 1, 2$ black holes clearly, one has to solve all linearized equations for physical perturbations numerically.

Accordingly, the criterion to determine whether a black hole is stable or not against the physical perturbations is whether the time evolution $e^{-i\omega t}$ of the perturbation is decaying or not. If $\omega_i < 0 (> 0)$, the black hole is stable (unstable), irrespective of any value of ω_r . However, it is a nontrivial task to carry out the stability of a scalarized charged black hole because this black hole comes out as not an analytic solution but a numerical solution. In order to develop the stability analysis, it is convenient to classify the linearized equations according to multipole index $l = 0, 1, 2, \dots$ because l determines number of physical fields at the axial and polar sectors.

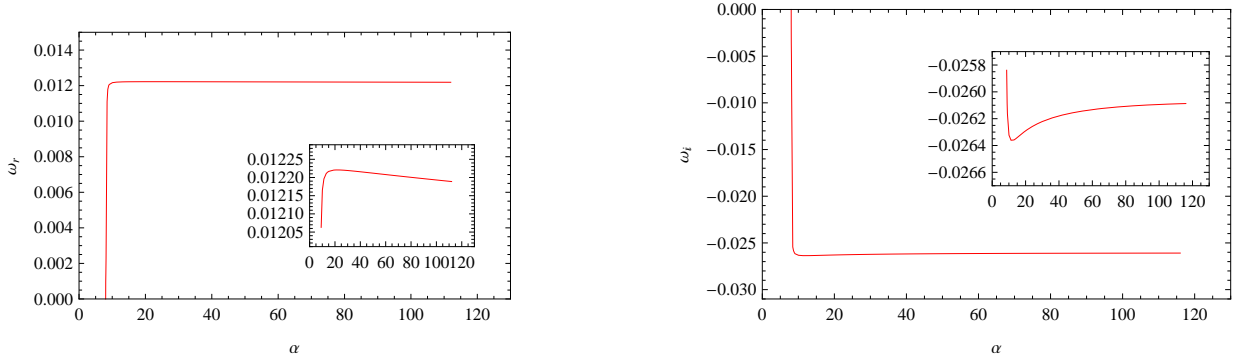


Figure 4: (Left) Real frequency ω_r and (Right) imaginary frequency ω_i for a scalar quasi-normal mode with $l = 0$ as a function of α around the $n = 0$ black hole. These start from $\alpha = 8.019$. The magnifications of the enclosed regions indicate the tendency for decreasing and increasing with respect to α .

4.1 $l = 0$ case: one DOF

For $l = 0$ (s -mode), the linearized equation obtained from the polar part is given entirely by a scalar equation ($\hat{S}_0^P = r\delta\phi_1$)

$$\left[\frac{d^2}{dr_*^2} + \omega^2 \right] \hat{S}_0^P - V_0^P(r, \alpha) \hat{S}_0^P = 0, \quad (34)$$

where the potential $V_0^P(r, \alpha)$ is given by [1]

$$V_0^P(r, \alpha) = \frac{N}{e^{2\delta} r^2} \left[1 - N - 2r^2 (\bar{\phi}')^2 + e^{-\alpha \bar{\phi}^2} Q^2 \left(\frac{2(-\alpha \bar{\phi} + r \bar{\phi}')^2 - \alpha - 1}{r^2} \right) \right]. \quad (35)$$

We display four scalar potentials $V_0^P(r, \alpha)$ in Fig. 3 for $l = 0$ case around the $n = 0$ black hole. The whole potentials are positive definite except that the $\alpha = 8.083$ case having negative region near the horizon does not represent instability really because it is near the threshold of instability. Actually, the $n = 0$ black hole is stable against the $l = 0$ (s -mode) scalar perturbation since the $n = 0$ case corresponds to the threshold of instability satisfying the condition of $\int_{r_+}^{\infty} dr [e^{\delta} V(r)/N(r)] > 0$. Although this condition does not rule out the possibility of unstable modes, one does not find any unstable modes. We confirm it from Fig. 4 that the imaginary frequency ω_i is negative for $\alpha \geq 8.019$, implying a stable $n = 0$ black hole. We observe that although ω_r and ω_i seem to be independent of α , it is not true. The magnifications of the enclosed regions show the tendency for decreasing and increasing with respect to α .

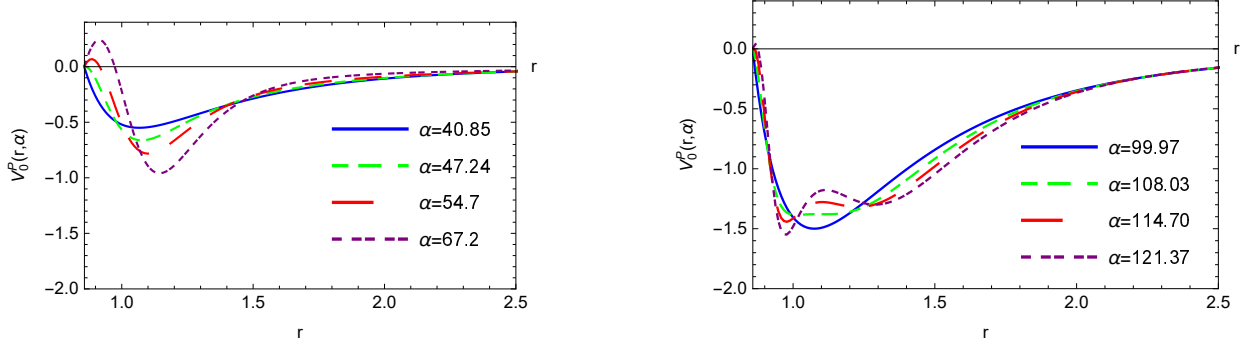


Figure 5: Four scalar potential graphs $V_0^P(r, \alpha)$ with $l = 0$ around (Left) $n = 1$ ($\alpha \geq 40.84$) black hole and (Right) $n = 2$ ($\alpha \geq 99.89$) black hole.

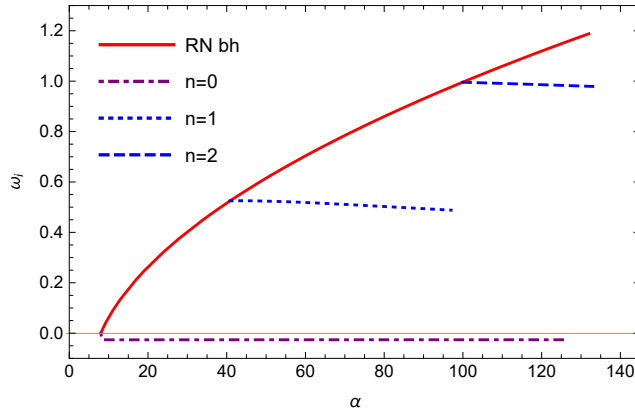


Figure 6: The positive imaginary frequency ω_i ($\omega_r = 0$) as function of α for the $l = 0$ scalar mode around the $n = 1, 2$ black holes. A red solid curve with $q = 0.7$ represents the quasinormal frequency of $l = 0$ scalar as function of α around the RN black hole [6], showing the instability of RN black holes. The red solid curve starts from the first bifurcation point at $\alpha = 8.019$. Attaching (Right) Fig.4 on Fig. 6 shows the negative imaginary frequency around the $n = 0$ black hole clearly.

Now let us turn to the stability issue of the $n = 1, 2$ black holes. We observe from Fig. 5 that $\int_{r_+}^{\infty} dr [e^{\delta} V(r)/N(r)] < 0$ for the $n = 1$ black hole, while all potentials are negative definite for the $n = 2$ black hole. This suggests that the $n = 1, 2$ black holes are unstable against the $l = 0$ (s -mode) scalar perturbation. Clearly, the instability could be found from Fig. 6 because their imaginary frequencies are positive. Here, the red curve denotes the instability (positive ω_i) of RN black hole as a function of α . Attaching (Right) Fig.4 on

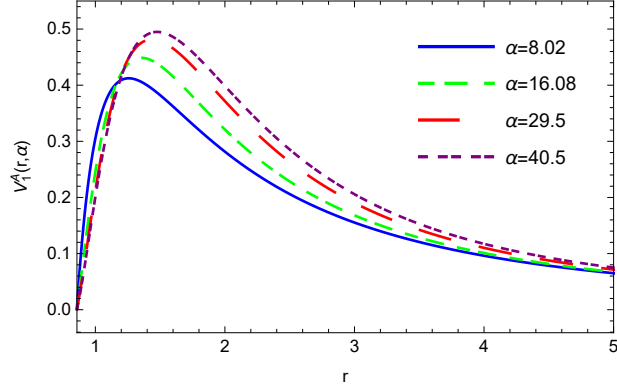


Figure 7: The positive potential $V_1^A(r, \alpha \geq 8.019)$ for axial $l = 1$ vector perturbation propagating around the $n = 0$ black hole.

Fig. 6 indicates the negative imaginary frequency around the $n = 0$ (stable) black hole. This instability may be regarded as the GL instability because it corresponds to the s -mode instability. Actually, Fig. 6 is regarded as our main result to show the (in)stability of $n = 0, 1, 2$ black holes.

Hereafter, we will perform the stability analysis for higher multipoles on the $n = 0$ black hole only because the $n = 1, 2$ black holes turned out to be unstable against the $l = 0(s)$ -mode perturbation. In other words, it is not meaningful to carry out a further analysis for the unstable $n = 1, 2$ black holes.

4.2 $l = 1$ case: three DOF

For $l = 1$ case, the axial linearized equation is given by

$$\left[\frac{d^2}{dr_*^2} + \omega^2 \right] \hat{F} - V_1^A(r, \alpha) \hat{F} = 0, \quad (36)$$

where the potential takes the form

$$V_1^A(r, \alpha) = -\frac{e^{-2\delta} N}{r^2} \left[N \left(4 - \alpha^2 \bar{\phi}^2 + \alpha r (\bar{\phi}^2)' - r^2 (\alpha - 4 + 2\alpha^2 \phi^2) (\bar{\phi}')^2 \right) - 6 + 4rN' + \alpha^2 \bar{\phi}^2 (1 - rN') \right] \quad (37)$$

We note that in the limits of $\bar{\phi}(r) \rightarrow 0$ and $\delta \rightarrow 0$, Eq.(37) reduces to the axial vector perturbed equation in the Einstein-Maxwell (EM) theory [23, 24]

$$V_{1\text{EM}}^A(r) = -\frac{N}{r^2} (4N - 6 + 4rN'). \quad (38)$$

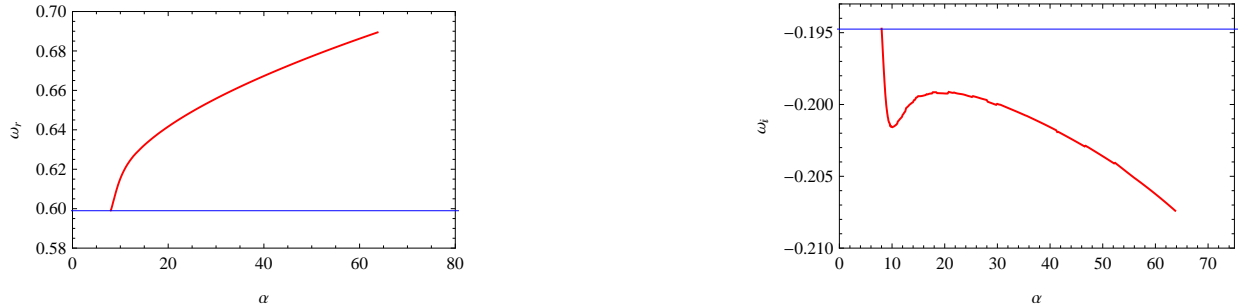


Figure 8: (Left) Real frequency and (Right) negative imaginary frequency as function of α for axial $l = 1$ vector mode around the $n = 0$ black hole. At $\alpha = 8.019$, one recovers the fundamental quasinormal frequency for the $l = 1$ EM mode around RN black hole (blue horizontal lines).

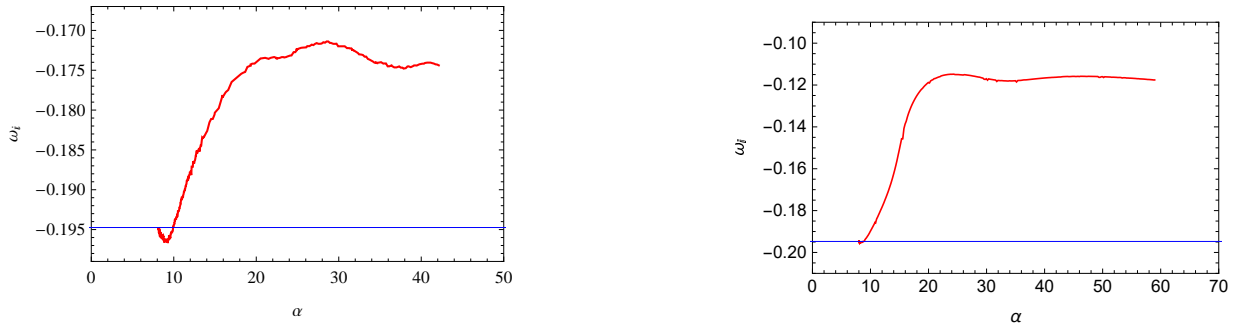


Figure 9: Imaginary frequencies as function of α for polar $l = 1$ vector-led mode (Left) and scalar-led mode (Right) around the $n = 0$ black hole.

We find from Fig. 7 that all potentials are positive definite for the $n = 0$ black hole. This means that the $n = 0$ black hole is stable against the axial $l = 1$ vector perturbation. We confirm it from Fig. 8 that ω_i is negative, indicating a stable black hole. Moreover, it is interesting to note that the quasinormal frequency at $\alpha = 8.019$ coincides with that for the $l = 1$ fundamental EM mode ($0.59896 - 0.19475i$) around the RN black hole [25, 26].

Finally, we find the vector-led and scalar-led modes around the $n=0$ black hole from the polar $l = 1$ linearized equations (28)-(33). We find from Fig. 9 that all ω_i of these modes around the $n = 0$ are negative, implying a stable black hole.



Figure 10: Imaginary frequencies as function of α for axial $l = 2$ vector-led mode (Left) and gravitational-led mode (Right) around the $n = 0$ black hole.

4.3 $l = 2$ case: five DOF

First of all, we consider the axial part because of its simplicity. The axial linearized equations are given by two coupled equations for Regge-Wheeler-Maxwell system (23) and (24) with $l = 2$. Solving these coupled equation with boundary conditions leads to negative quasinormal frequencies $\omega_i < 0$ for $l = 2$ vector-led and gravitational-led modes around the $n = 0$ black hole (see Fig. 10), implying stable black hole. Here we find the fundamental frequency of $1.07302 - 0.197542i$ for the $l = 2$ vector-led mode around the RN black hole in the EM theory [25, 26]. We note that the $l = 2$ fundamental frequency of $0.784997 - 0.179809i$ (for gravitational-led mode around the RN black hole in the EM theory) plays the role of a starting point for the $n = 0$ black hole.

Now, the polar $l = 2$ linearized equations are given by Eqs.(28)-(33) with $l = 2$. Here we have three modes: vector-led, gravitational-led, and scalar-led modes. We find from Figs. 11 and 12 that all ω_i are negative, implying the stable $n = 0$ black hole. It is worth noting that the $l = 2$ fundamental frequencies of vector-led and gravitational-led modes around the RN black hole in the EM theory take the same values as in the axial case [27]. For the polar $l = 2$ scalar-led mode, the quasinormal frequency starts from $0.9923 - 0.1834i$ for $\alpha = 8.019$.

5 Summary

In this work, we performed the stability analysis of the scalarized charged black holes in the EMS theory by computing quasinormal mode spectrum. This is a nontrivial task and

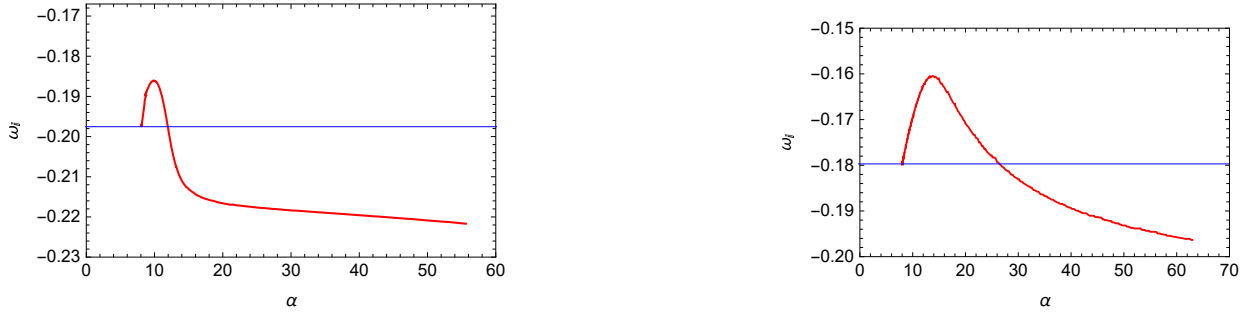


Figure 11: Imaginary frequencies as function of α for polar $l = 2$ vector-led mode (Left) and gravitational-led mode (Right) around the $n = 0$ black hole.

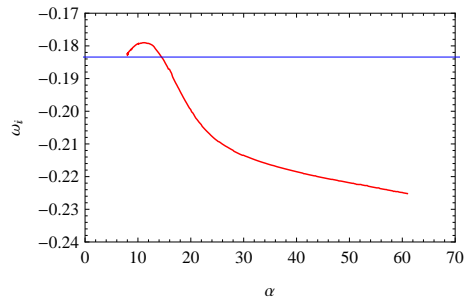


Figure 12: Imaginary frequency for polar $l = 2$ scalar-led mode around the $n = 0$ black hole.

completing it takes a long time because these black holes are found in numerically.

We have shown that the $n = 1(\alpha \geq 40.84)$, $2(\alpha \geq 99.89)$ excited black holes are unstable against the $s(l = 0)$ -mode scalar perturbation only, while the $n = 0(\alpha \geq 8.019)$ fundamental black hole is stable against all scalar-vector-tensor perturbations. In the former case, the instability of the $n = 1, 2, \dots$ black holes is regarded as the Gregory-Laflamme instability because it arose from the $s(l = 0)$ mode with an effective mass term. In the latter, we found negative quasinormal frequencies ($\omega_i < 0$) of $9 = 1(l = 0) + 3(l = 1) + 5(l = 2)$ physical modes around $n = 0$ black hole. We could not find any unstable modes from the $l = 0, 1, 2$ scalar-vector-tensor perturbations around the $n = 0$ black hole, as in the RN black hole [6]. Even though we have carried out the stability analysis on the $n = 0, 1, 2$ black holes, we expect to find from Fig. 5 that the other higher excited ($n = 3, 4, 5, \dots$) black holes are unstable against the $s(l = 0)$ -mode scalar perturbation. This picture is consistent with other scalarized black holes without charge found in the ESGB theory by making use of

spherically symmetric perturbations [17].

Acknowledgments

We are grateful to Yunqi Liu for useful discussions. This work was supported by the National Research Foundation of Korea (NRF) grant funded by the Korea government (MOE) (No. NRF-2017R1A2B4002057).

References

- [1] C. A. R. Herdeiro, E. Radu, N. Sanchis-Gual and J. A. Font, Phys. Rev. Lett. **121**, no. 10, 101102 (2018) doi:10.1103/PhysRevLett.121.101102 [arXiv:1806.05190 [gr-qc]].
- [2] F. J. Zerilli, Phys. Rev. D **9**, 860 (1974). doi:10.1103/PhysRevD.9.860
- [3] V. Moncrief, Phys. Rev. D **9**, 2707 (1974). doi:10.1103/PhysRevD.9.2707
- [4] V. Moncrief, Phys. Rev. D **10**, 1057 (1974). doi:10.1103/PhysRevD.10.1057
- [5] V. Moncrief, Phys. Rev. D **12**, 1526 (1975). doi:10.1103/PhysRevD.12.1526
- [6] Y. S. Myung and D. C. Zou, arXiv:1808.02609 [gr-qc].
- [7] H. O. Silva, J. Sakstein, L. Gualtieri, T. P. Sotiriou and E. Berti, Phys. Rev. Lett. **120**, no. 13, 131104 (2018) doi:10.1103/PhysRevLett.120.131104 [arXiv:1711.02080 [gr-qc]].
- [8] G. Antoniou, A. Bakopoulos and P. Kanti, Phys. Rev. Lett. **120**, no. 13, 131102 (2018) doi:10.1103/PhysRevLett.120.131102 [arXiv:1711.03390 [hep-th]].
- [9] D. D. Doneva and S. S. Yazadjiev, Phys. Rev. Lett. **120**, no. 13, 131103 (2018) doi:10.1103/PhysRevLett.120.131103 [arXiv:1711.01187 [gr-qc]].
- [10] R. Gregory and R. Laflamme, Phys. Rev. Lett. **70**, 2837 (1993) doi:10.1103/PhysRevLett.70.2837 [hep-th/9301052].
- [11] Y. S. Myung and D. C. Zou, Phys. Rev. D **98**, no. 2, 024030 (2018) doi:10.1103/PhysRevD.98.024030 [arXiv:1805.05023 [gr-qc]].
- [12] B. Whitt, Phys. Rev. D **32**, 379 (1985). doi:10.1103/PhysRevD.32.379
- [13] Y. S. Myung, Phys. Rev. D **88**, no. 2, 024039 (2013) doi:10.1103/PhysRevD.88.024039 [arXiv:1306.3725 [gr-qc]].
- [14] H. L. A. Perkins, C. N. Pope and K. S. Stelle, Phys. Rev. D **96**, no. 4, 046006 (2017) doi:10.1103/PhysRevD.96.046006 [arXiv:1704.05493 [hep-th]].
- [15] K. S. Stelle, Int. J. Mod. Phys. A **32**, no. 09, 1741012 (2017). doi:10.1142/S0217751X17410123

- [16] D. D. Doneva, S. S. Yazadjiev, K. D. Kokkotas and I. Z. Stefanov, *Phys. Rev. D* **82**, 064030 (2010) doi:10.1103/PhysRevD.82.064030 [arXiv:1007.1767 [gr-qc]].
- [17] J. L. Blzquez-Salcedo, D. D. Doneva, J. Kunz and S. S. Yazadjiev, *Phys. Rev. D* **98**, no. 8, 084011 (2018) doi:10.1103/PhysRevD.98.084011 [arXiv:1805.05755 [gr-qc]].
- [18] D. Garfinkle, G. T. Horowitz and A. Strominger, *Phys. Rev. D* **43**, 3140 (1991) Erratum: [*Phys. Rev. D* **45**, 3888 (1992)]. doi:10.1103/PhysRevD.43.3140, 10.1103/PhysRevD.45.3888
- [19] C. Pacilio and R. Brito, *Phys. Rev. D* **98**, no. 10, 104042 (2018) doi:10.1103/PhysRevD.98.104042 [arXiv:1807.09081 [gr-qc]].
- [20] S. Chandrasekhar, *Proc. Roy. Soc. Lond. A* **365**, 453 (1979). doi:10.1098/rspa.1979.0028
- [21] J. L. Blzquez-Salcedo, C. F. B. Macedo, V. Cardoso, V. Ferrari, L. Gualtieri, F. S. Khoo, J. Kunz and P. Pani, *Phys. Rev. D* **94**, no. 10, 104024 (2016) doi:10.1103/PhysRevD.94.104024 [arXiv:1609.01286 [gr-qc]].
- [22] G. Dotti and R. J. Gleiser, *Class. Quant. Grav.* **22**, L1 (2005) doi:10.1088/0264-9381/22/1/L01 [gr-qc/0409005].
- [23] E. W. Leaver, *Phys. Rev. D* **41**, 2986 (1990). doi:10.1103/PhysRevD.41.2986
- [24] E. Berti and K. D. Kokkotas, *Phys. Rev. D* **71**, 124008 (2005) doi:10.1103/PhysRevD.71.124008 [gr-qc/0502065].
- [25] H. T. Cho, A. S. Cornell, J. Doukas, T. R. Huang and W. Naylor, *Adv. Math. Phys.* **2012**, 281705 (2012) doi:10.1155/2012/281705 [arXiv:1111.5024 [gr-qc]].
- [26] J. Matyjasek and M. Opala, *Phys. Rev. D* **96**, no. 2, 024011 (2017) doi:10.1103/PhysRevD.96.024011 [arXiv:1704.00361 [gr-qc]].
- [27] V. Cardoso, C. F. B. Macedo, P. Pani and V. Ferrari, *JCAP* **1605**, no. 05, 054 (2016) doi:10.1088/1475-7516/2016/05/054 [arXiv:1604.07845 [hep-ph]].